

The stabilizer ground state and applications to quantum simulation

Yuping Mao,¹ Chang Chen,¹ Jiaxing Feng,¹ Yimeng Mao,¹ and Tim Byrnes^{2,3,4,5}

¹*School of Science, Huzhou University, Huzhou, Zhejiang 313000, China*

²*New York University Shanghai; NYU-ECNU Institute of Physics at NYU Shanghai,
567 West Yangsi Road, Pudong, Shanghai 200126, China*

³*State Key Laboratory of Precision Spectroscopy, School of Physical and Material Sciences,
East China Normal University, Shanghai 200062, China*

⁴*Center for Quantum and Topological Systems (CQTS),*

NYUAD Research Institute, New York University Abu Dhabi, UAE

⁵*Department of Physics, New York University, New York, NY, 10003, USA*

(Dated: December 2025)

The stabilizer ground state is defined as the lowest energy stabilizer state with respect to a given Hamiltonian. In many cases it is highly degenerate and does not give a unique stabilizer state. We define the optimal stabilizer ground state as the stabilizer ground state which has the highest fidelity with the true ground state. This is useful in quantum simulation contexts as it allows for a Clifford circuit approximation of a ground state that can be further refined towards the true ground state. We show how the optimal stabilizer ground state may be evaluated. We show applications of this state in the context of measurement-based deterministic imaginary time evolution (MITE), which converges to the ground state with high efficiency. By classically selecting the optimal stabilizer generator group and employing the stabilizer tableaux formalism, the method prepares the corresponding stabilizer ground state with maximal fidelity. The identification and refinement of this generator group are performed using a genetic algorithm tailored to the structure of the target Hamiltonian. The complexity analysis further demonstrates that algorithm's quantum resource cost scales polynomially with system size, highlighting its high efficiency and potential quantum advantage.

I. INTRODUCTION

In recent years, quantum computing has experienced rapid growth [1–6]. With the improvements in quantum hardware, a broad range of quantum applications are gradually moving towards practical implementation, particularly in the field of quantum simulation [7–11]. The primary objective of quantum simulation is to reproduce the behavior of physical systems using controllable quantum systems. This approach has a variety of applications in many fields, such as quantum chemistry, high-energy physics, and condensed matter physics [12–18]. A common feature among these applications is that the target problems involve quantum many-body systems, which can be encoded onto the quantum computer [19–21]. Compared with classical computation, quantum simulation has the potential to exhibit significantly higher efficiency in solving such problems [22].

Quantum state preparation plays an essential role in both quantum simulation [23, 24] and quantum computation [25, 26]. The importance of quantum state preparation is twofold. Initial state preparation is an inevitable step for digital quantum simulation, such as phase estimation algorithm [27]. For these methods, preparing an initial state with minimal error can significantly improve both efficiency and accuracy of quantum algorithms [28–31]. Consequently, quantum state preparation remains one of the central purposes in quantum simulation and quantum computation [7, 32]. Several general quantum state preparation methods have been proposed, including variational quantum eigensolver (VQE)-

based approaches [33, 34], quantum compressed sensing-based encoding [35–37], and random projection methods [38]. For some particular class of systems, numerous specialized state preparation protocols have been developed, such as those for Fermi systems [23, 39, 40], molecular systems [24, 41], lattice models [42]. While these algorithms provide broadly applicable state preparation strategies, they are typically resource-demanding, posing significant challenges for noisy intermediate-scale quantum (NISQ) devices. Stabilizer states are a class of quantum state which are broadly used in quantum computation [43] and quantum simulation [44, 45]. Stabilizer ground states are a special subclass of stabilizer states that minimizes the stabilizer group energy [46]. The advantages of stabilizer ground states include their efficient classical description and inherent compatibility with fault-tolerant quantum operations. For an N -qubit system, a stabilizer state is uniquely specified by a set of at most N independent Pauli operators [47, 48]. The states can be efficiently prepared using Clifford circuits, which are naturally compatible with quantum error correction protocols [49, 50].

Imaginary-time evolution (ITE) method is a widely used approach for quantum state preparation [51, 52]. There are some typical algorithm like quantum imaginary time evolution and variational time evolution algorithms. The quantum imaginary time evolution (QITE) scheme iteratively applies a small-step non-unitary operator $e^{-\Delta\beta H}$ to an initial state $|\psi\rangle$, whose cumulative effect approximates imaginary time evolution process. Through this mechanism, QITE has been developed as a practical framework for preparing quantum

states on quantum computers [53]. Variational imaginary time evolution (VITE) scheme employs McLachlan variational principle to map imaginary time evolution process onto a classical optimization problem over a parameterized quantum circuit $|\psi(\theta)\rangle$ [52]. Owing to its hybrid classical-quantum nature, VITE is well suited for NISQ devices and has attracted considerable interests [54–56]. Recently Measurement-based deterministic imaginary time evolution (MITE) [57] has been proposed as an alternative approach to implement imaginary time evolution through weak measurements. The scheme approximates imaginary time evolution using weak measurements constructed via Suzuki-Trotter decomposition [58–60], thereby transforming infinitely long time evolution into a sequence of random weak measurements. When the MITE scheme yields a random outcome that fails to satisfy the energy threshold, a unitary operation is implemented to the system. MITE has demonstrated strong potential for quantum state preparation [61, 62], including the preparation of AKLT state [63] and super-singlet state [61].

In this paper, we focus on the goal of efficient ground-state preparation. With the principle of weak measurements, we optimize the MITE scheme by introducing a pre-prepared stabilizer ground state with the highest fidelity. This means the first step of this method is to generate a stabilizer state which has the lowest energy and highest fidelity with respect to Hamiltonian’s ground state. Due to the Gottesmann-Knill theorem, this stabilizer ground state can be efficiently prepared using classical computation. We implement The optimal stabilizer ground state as the initial state of the MITE scheme. Due to its high fidelity, the required depth of weak measurement circuit is dramatically reduced. Furthermore, the lowest stabilizer-group energy can be a suitable candidate for energy threshold in MITE, enabling the implementation of this scheme without prior knowledge of exact ground-state energy and first excited-state energy. With these two optimizations, the efficiency and the universality of MITE scheme are markedly improved.

This paper is structured as follows. In Sec. II, we briefly review the stabilizer formalism for stabilizer ground states and introduce the criterion of magic state witness, which provides the definition and method we employed in this work [46, 50]. In Sec. III, we present the construction of a method for preparing stabilizer ground state using the approach, which is particularly effective for small-scale systems. In Sec. IV, we describe a general method for selecting the optimal stabilizer generator set and preparing the stabilizer ground state. Sec. V recalls the MITE scheme and explains how it can be adapted to evolve with the stabilizer ground state as the initial state. In Sec. V.3, we analyze the computational complexity and convergence error of this hybrid MITE scheme. Sec. V.4 provides numerical simulations demonstrating that the hybrid scheme achieves higher efficiency compared to the original MITE scheme. Finally, Sec. VI is the summary of main results in this work.

II. STABILIZER GROUND STATE AND RESOURCE OF MAGIC STATE WITNESS

In this section, we review the stabilizer state’s definition and Robustness of magic, which quantifies the non-stabilizerness of pure state and introduce the concept of a stabilizer ground state.

II.1. Stabilizer state

The stabilizer formalism is a practical framework for characterizing quantum state, originally introduced by Gottesman [64, 65]. For an N -qubit system, a stabilizer state $|\psi_s\rangle$ is stabilized by a stabilizer generator group G , which is formed by the tensor product of Pauli operators

$$G = \{g_1, g_2, \dots, g_n\}, \quad (1)$$

$$g_i |\psi_s\rangle = |\psi_s\rangle. \quad (2)$$

Stabilizer states plays a central role in quantum error correction and fault-tolerant quantum computation [66–68].

The set of pure N -qubit stabilizer states is denoted by $S_n = \{\sigma_i\}$ where each σ_i is represented in the density matrix form as $\sigma_i = |\psi_s^{(i)}\rangle\langle\psi_s^{(i)}|$. A general stabilizer state can be defined as the mixture of pure stabilizer states

$$\rho = \sum_i x_i \sigma_i, \quad (3)$$

where x_i are (potentially negative) real numbers satisfying $\sum_i x_i = 1$.

II.2. Robustness of Magic

Stabilizer formalism provides an effective framework for simulating Clifford gates. It can be extended to universal quantum computation when non-Clifford gates are added. However, one of the main challenges lies in the efficient incorporation of non-Clifford gates within the stabilizer framework. Robustness of Magic (RoM) [50] quantifies the degree to which a quantum state cannot be written as a stabilizer state.

For a general stabilizer state ρ , RoM’s general definition is

$$R(\rho) = \min_x \left\{ \sum_i |x_i|; \rho = \sum_i x_i \sigma_i \right\}. \quad (4)$$

RoM can be reformulated as a linear programming problem as

$$R(\rho) = \min \|x\|_1 \text{ subject to } Ax = b, \quad (5)$$

where $\|x\|_1 = \sum_i |x_i|$, $b_i = \text{Tr}(P_i \rho)$, and $A_{j,i} = \text{Tr}(P_j \sigma_i)$. Here b_i is the vector of expectation values for

each Pauli string whose dimension grows with the scale of quantum system. The effects x_i denotes the quasi-probability parameter for the mixed state ρ , which may takes negative value.

In Eq. (5), the non-stabilizerness criterion works as $R(\rho) \geq 1$. $R(\rho) > 1$ is the necessary and sufficient criterion for witness of magic, while for any convex mixture of stabilizer states, $R(\rho) = 1$. RoM provides a boundary between classical and magic states, and shows great impact for quantifying quantum efficiency. It is formally a magic monotone for arbitrary states [50].

A is a full row-rank matrix whose Moore-Penrose inverse A^\dagger can be written as

$$A^\dagger = \sum_m G_m,$$

$$G_m = \sum_{n=1}^{4^N} g_{mn}.$$

By looking for the matrix A^\dagger in the respect to the stabilizer formalism, we found that G_m corresponds to a set of N -qubit Pauli group \mathcal{P} , with sign ± 1 ensuring the normal-closure property. Each G_m has 2^N non-zero elements which denotes Pauli strings forming a stabilizer subgroup, which corresponds to the N -qubit system's maximally commuting stabilizer subgroup which contains 2^N Pauli strings[69].

We define the corresponding stabilizer generator group \mathcal{G}_m as the minimal generating set of N independent, mutually commuting Pauli strings whose products all nonzero terms of G_m . Due to the nature of stabilizer formalism, each stabilizer generator group \mathcal{G}_m uniquely stabilizes a single stabilizer state $|\psi_s\rangle$.

These definitions can be clarified by considering the single-qubit case. The single-qubit Pauli group consists of the Pauli operators $\mathcal{P} = \{\pm I, \pm X, \pm Y, \pm Z\}$, which corresponds to all the stabilizer generator groups $\{G_1, \dots, G_6\}$. Each stabilizer generator group contains two nontrivial elements, consistent with the general relation $|G_m| = 2^N$ for an N -qubit stabilizer group.

For single-qubit case, the independent stabilizer generator group coincides with the full stabilizer group, i.e., $\mathcal{G}_m = G_m$. Consequently, an N -qubit stabilizer state $|\psi_s\rangle$ can be uniquely specified by N independent stabilizer generators.

II.3. Stabilizer ground state

The stabilizer ground state is defined as the stabilizer state which minimizes the energy expectation value of given Hamiltonian H , i.e.,

$$|\psi_{SGS}\rangle = \arg \min_{|\psi_s^{(i)}\rangle} \langle \psi_s^{(i)} | H | \psi_s^{(i)} \rangle, \quad (6)$$

where $|\psi_s^{(i)}\rangle$ denotes an N -qubit stabilizer state, as defined above.

It has been shown that for a 1D local Hamiltonian, the stabilizer ground state can be obtained with linearly scaled computational complexity [46]. Furthermore, the stabilizer ground state can be an efficient initial state for variational quantum algorithms (VQAs) [70].

In general, the stabilizer ground state is not unique. Accordingly, we define the N -qubit stabilizer ground-state manifold as

$$\mathcal{S}_{SGS}^{(N)} = \left\{ |\psi\rangle \left| \langle \psi | H | \psi \rangle = \min_{|\psi_s^{(i)}\rangle} \langle \psi_s^{(i)} | H | \psi_s^{(i)} \rangle \right. \right\}, \quad (7)$$

where the minimization is taken over all N -qubit stabilizer states.

III. OPTIMAL STABILIZER GROUND STATE

We now formulate a method to derive the optimal stabilizer ground state, which can be efficiently obtained within Gottesman-Knill framework. The advantage of the stabilizer formalism lies in its high-efficiency preparation based on Clifford gates and classical post-processing. Here we clarify the reason of introducing the optimal stabilizer ground state.

III.1. Definition

For stabilizer non-unique cases, as multiple states can share the same lowest energy while exhibiting significantly different fidelities with respect to the true ground state. Such stabilizer ground state is no longer a reliable initial state candidate for quantum algorithms.

We therefore define the optimal stabilizer ground state $|\psi_{OSGS}\rangle$ as the stabilizer state that has both the lowest stabilizer-group energy and the highest fidelity with respect to the true ground state,

$$|\psi_{OSGS}\rangle = \arg \max_{|\psi_{SGS}\rangle \in \mathcal{S}_{SGS}^{(N)}} |\langle E_0 | \psi_{SGS} \rangle|^2. \quad (8)$$

Such optimal stabilizer ground state has both the lowest stabilizer-group energy and the highest fidelity with respect to the true ground state. The optimal stabilizer ground state can be a promising initial state for the ITE scheme.

III.2. Evaluating the OSGS

We introduce the method for seeking the optimal stabilizer ground state based on the framework of robustness of magic(RoM).

Consider an N -qubit system, the Hamiltonian H can be expressed in the Pauli operator basis as

$$H = \sum_{P \in \mathcal{S}} h_p P, \quad (9)$$

where $\mathcal{S} \subseteq \mathcal{P}$ and $\mathcal{P} = \{\bigotimes_{j=1}^N p_j | p_j \in \{I_j, X_j, Y_j, Z_j\}\}$ is a N -qubit Pauli group which includes the full set of Pauli strings with $|\mathcal{P}| = 4^N$, \mathcal{S} is a subset of Pauli Strings which in the Hamiltonian H with non-zero factors $h_P \in \mathbb{R}$.

To characterize the contribution of each Pauli operator to Hamiltonian H , we define the candidate generator set \mathbf{b} as

$$\mathbf{b} = \text{Tr}(\mathcal{P}H), \quad (10)$$

The non-zero components of \mathbf{b} identify the Pauli operators that work as candidate stabilizer generators in the given Hamiltonian.

The lowest stabilizer-group energy is defined as

$$E_{\min}^S = \min_{j \in \{1, 2, \dots, m\}} \frac{x_j}{2^N}, \quad \text{where } x = A^\dagger \mathbf{b}. \quad (11)$$

This formula can be regarded as a direct analogue of Eq. (5). For a full row rank A , the Moore-Penrose pseudoinverse A^\dagger acts as its left inverse. Physically, E_{\min}^S quantifies the lowest attainable energy within the stabilizer subspace compatible with Hamiltonian H .

We will prove Eq. (11) provides the criterion for determining the lowest stabilizer-group energy. For Hamiltonian in the form Eq. (9), the candidate generator set can be calculated as

$$\begin{aligned} b_i &= \sum_p h_p \text{Tr}(P_i \cdot P_p) \\ &= 2^N \sum_p h_i \delta_{ip} \\ &= 2^N h_i, \end{aligned} \quad (12)$$

where h_i denotes the weight factor corresponding to the Pauli string P_i in the Hamiltonian H . The non-zero trace result happens only when $P_i = P_p$, since their product reduces to the identity operator $I^{\otimes N}$, yielding a trace value of 2^N . By normalizing the weight factor $2^N h_i$ to 1, the non-zero terms of candidate generator set \mathbf{b} can be mapped onto the Hamiltonian set \mathcal{S} . This establishes a one-to-one correspondence between the non-zero Pauli terms in H and the stabilizer generator candidates. $A^\dagger \mathbf{b}$ in Eq. (11) can be written as

$$\begin{aligned} x_m &= (A^\dagger \mathbf{b})_m = G_m \sum_p 2^N h_p \\ &= 2^N \sum_p \sum_{n=1}^{2^N} \text{sgn}(g_{mn}) h_p \delta_{np} \\ &= 2^N \sum_p \text{sgn}(g_{mp}) h_p, \end{aligned} \quad (13)$$

where $\text{sgn}(g_{mp}) \in \{\pm 1\}$ is the sign of the corresponding stabilizer generator component. Substituting Eq. (13) into Eq. (11) yields the expression for the lowest stabilizer-group energy

$$E_{\min}^S = \min_{j \in \{1, 2, \dots, m\}} \sum_p \text{sgn}(g_{jp}) h_p. \quad (14)$$

Equation (14) satisfies the definition of stabilizer group energy (see Appendix A). Once the lowest stabilizer-group energy is obtained, the corresponding stabilizer generator group G_{\min} can be located. However, as conveyed earlier, the stabilizer generator group obtained by this method is not always unique. In fact, these non-unique stabilizer ground states lie within the same sub-Hilbert space and can be transferred into one another through Clifford operations. To ensure a high-quality initial state for MITE scheme, we therefore define the optimal stabilizer ground state which has the highest fidelity to the true ground state.

Then we describe how to identify the stabilizer generator group corresponding to The optimal stabilizer ground state. We define the stabilizer subgroup which takes the lowest stabilizer-group energy as

$$G_{\min} = \{G_{\min}^{(1)}, \dots, G_{\min}^{(Q)}\},$$

in which each $G_{\min}^{(q)}$ denotes a Pauli group that corresponding to the lowest stabilizer-group energy. By removing the non-zero terms, it can be expressed as $G_{\min}^{(q)} = \{g_1^{(q)}, \dots, g_{2^N}^{(q)}\}$, where $g_n^{(q)}$ represents the n -th stabilizer generator in $G_{\min}^{(q)}$. The $G_{\min}^{(q)}$ we define here is a maximal commuting subgroup for an N -qubit system. The corresponding independent stabilizer generator groups can be defined as $\mathcal{G}_{\min} = \{G_{\min}^{(1)}, \dots, G_{\min}^{(q)}\}$ in which $|\mathcal{G}_{\min}^{(q)}| = N$.

By comparing the stabilizer subgroup $G_{\min}^{(i)}$ within G_{\min} , we find that they share some common Pauli operators. We define the common stabilizer generator subgroup as

$$G_{\text{com}} := \left\langle \bigcap_{i=1}^Q G_{\min}^{(i)} \right\rangle, \quad I^{\otimes N} \notin G_{\text{com}}. \quad (15)$$

We exclude $I^{\otimes N}$ since it is a trivial element shared by all the lowest-energy stabilizer subgroups. It follows that G_{com} is also a subgroup of Hamiltonian set \mathcal{S} .

To further classification, we construct the sub-Hamiltonian H_{sub} by removing the Pauli terms contained in G_{com} from the original Hamiltonian H , such that it becomes

$$H_{\text{sub}} = \sum_a h_a P_a, P_a \in B \setminus G_{\text{com}}. \quad (16)$$

The process of identifying the optimal stabilizer generator group can then be divided into the following two steps. We will demonstrate them in Appendix B).

(1) Define the filter function $\xi(G_{\min}^{(i)}, H)$ as:

$$\xi(G_{\min}^{(i)}, H) = \begin{cases} 1, & \text{if } \exists j \in \{1, \dots, N\}, [g_j^{(i)}, H] = 0 \\ 0, & \text{if } \forall j \in \{1, \dots, N\}, [g_j^{(i)}, H] \neq 0 \end{cases}, \quad (17)$$

where $g_j^{(i)} \in \mathcal{G}_{\min}^{(i)}$ denotes the j -th stabilizer generator within the stabilizer generator group $\mathcal{G}_{\min}^{(i)}$. The filter function tests the commutation relation between Hamiltonian H and each generator in group $\mathcal{G}_{\min}^{(q)}$, and allows to keep $\mathcal{G}_{\min}^{(q)}$ that include at least one commute generator. Thus

$$\mathcal{G}_{\text{keep}} = \{\mathcal{G}_{\min}^{(i)} \in \mathcal{G}_{\min} \mid \xi(\mathcal{G}_{\min}^{(i)}, H) = 1\}. \quad (18)$$

This procedure will effectively reduce the degeneracy of the lowest stabilizer-group energy.

(2) For the sub-Hamiltonian H_{sub} , the remaining stabilizer generators can be extracted using a similar method. By constructing candidate generator set \mathbf{b}^{sub} for H_{sub} , selecting the lowest-energy stabilizer group $\mathcal{G}_{\min}^{\text{sub}}$, and evaluating its commutation relations with the original Hamiltonian H using filter function $\xi(\mathcal{G}_{\min}^{\text{sub}}, H) = 1$, we find the corresponding stabilizer subgroup $\mathcal{G}_{\text{keep}}^{\text{sub}}$. Finally, the independent stabilizer generator group with the lowest stabilizer-group energy and the highest fidelity will be chosen as the optimal stabilizer generator group \mathcal{G}^{op}

$$\mathcal{G}^{\text{op}} = \{\mathcal{G}_{\min}^{(i)} \mid \mathcal{G}_{\text{keep}} \cap \mathcal{G}_{\text{keep}}^{\text{sub}} \neq \emptyset\}. \quad (19)$$

When system's ground state is degenerate, \mathcal{G}^{op} will contain more than one generator groups. However, these groups possess the same fidelity with the respect to the true ground state of Hamiltonian. So there is no need to identify them, either group can be the optimal choice.

Once the optimal independent generator group is obtained, the stabilizer ground state can be prepared using stabilizer tableau representation [48, 71]. By encoding both initial state's generator group and stabilizer ground state's generator group in tableau form and applying proper column transformations, we can derive the quantum circuit to derive the optimal stabilizer ground state using Clifford operations. Based on this approach, several efficient stabilizer simulators have been developed [72, 73].

With above procedure, we obtain a general method for preparing the stabilizer ground state. It might have broad potential applications as it's the stabilizer state which is closest to Hamiltonian's ground state and can be efficiently generated with classical computation assisted by Clifford gates. The primary advantage of such a state lies in its highly efficiency for state preparation: It substantially shortens the required quantum circuit depth and reduces the consumption of quantum resource. Although this method is based on the stabilizer formalism, it doesn't mean that it is limited to the Clifford systems. Instead, our method tries to find out the most suitable Clifford circuit that approximates the given non-Clifford system. Constructing a stabilizer-based approximation for non-Clifford systems may influence the fidelity and convergence rate of the resulting stabilizer ground state, but the method remains effective in achieving reliable ground-state preparation. There are also some methods of quantifying and simulating non-Clifford systems with Clifford circuit [50, 74].

IV. SELECTION OF OPTIMAL STABILIZER GENERATOR GROUP FOR LARGER SYSTEMS

In previous section, we have presented a general method to derive the optimal stabilizer ground state for small system size. The dimension of A matrix limits the scalability of quantum system [50]. The matrix A enumerates all possible maximally commuting stabilizer subgroups which has the dimension of $(2^N \prod_n (2^n + 1)) \times 4^N$. For example, the RoM using standard methods can only be calculated up to $N = 5$ qubits. Using more advanced methods [75] it is possible to push the sizes to $N = 8$, but eventually the problem becomes intractable.

With such A matrix, we can find the lowest stabilizer-group energy via Eq. (13). However, the exponential computational growth restricts the feasibility of matrix A to small-scale systems. For large systems, finding A is an NP-hard problem which cannot be efficiently solved. To address this problem, we develop a method to identify the optimal stabilizer generator group with the lowest stabilizer-group energy.

Similar to the previous procedure, the candidate generator set \mathbf{b} is computed from the given Hamiltonian H with Eq. (10). We note that in \mathbf{b} , only the elements corresponding to $P_p = P_i$ are non-zero. For the aim of searching for the optimal stabilizer subgroup that has the lowest stabilizer group energy, G^{op} must satisfy

$$x_{\min} = G^{\text{op}} \mathbf{b}, \quad (20)$$

where we define G^{op} 's corresponding optimal independent stabilizer generator as \mathcal{G}^{op} . The unique identification of G^{op} depends solely on locating \mathcal{G}^{op} . Hence, the problem of identifying G^{op} can be reformulated as finding the independent stabilizer generator group \mathcal{G}^{op} .

As we shown in Eq. (13), only the Pauli terms satisfying $P_i = P_p$ contribute non-zero values. To satisfy Eq. (20), it is necessary to first identify which elements of the candidate generator set \mathbf{b} contribute to the stabilizer group energy. In Eq. (13), the stabilizer group energy $E(H)$ is expressed as a weighted sum of the expectation values of stabilizer generators defined by the candidate generator set \mathbf{b} . Accordingly, the maximum stabilizer group energy satisfies

$$E_{\max}^S = \max \sum_p |b_p|, \text{ where } P_p \in \mathcal{G}^{\text{op}}. \quad (21)$$

Similarly, the minimal stabilizer-group energy E_{\min}^S can be obtained by flipping the phases of stabilizer generators. It is determined by the Pauli strings of the stabilizer generators, while non-stabilizer terms in the candidate generator set \mathbf{b} do not affect the stabilizer group energy $E(H)$.

With the understanding of how candidate generator set \mathbf{b} contributes to the stabilizer-group energy $E(H)$, the problem of finding the optimal generator group can be reformulated as the task like how to select a maximal commuting Pauli string group that minimizes the stabilizer-group energy $E_{\min}^S(H)$.

The candidate generator set \mathbf{b} contains p nonzero elements, each corresponding to a Pauli string with weighted factor $2^N h_p$. The commutation relation between each Pauli strings' pair in \mathbf{b} which can be characterized by the commutation matrix C , defined as

$$C_{ij} = [b_i, b_j], \quad b_i, b_j \in \mathbf{b}. \quad (22)$$

The commutation matrix C is symmetric with zero diagonal entries and can be mapped onto the adjacency matrix of a weighted undirected graph that encodes the commutation relations among the Pauli strings. In this framework, the problem of finding the lowest stabilizer-group energy is identical to identifying the maximal cliques in the corresponding undirected graph[76].

Although finding the maximal cliques is an NP-hard problem when seeking exact solutions for large-scale systems, obtaining approximate solutions within polynomial time is feasible[77]. Various classical algorithms have been developed for such problems, including greedy algorithm[78], local search algorithm[79], and neutral network-based methods[80]. From the quantum algorithm perspective, the maximal cliques problem belongs to the class of combinatorial optimization problems that can be mapped onto the Ising model. Consequently, quantum algorithms such as quantum annealing, Quantum Approximate Optimization Algorithm(QAOA) can be applied on these problems[81, 82].

Evolutionary algorithms, such as genetic algorithm, have also been widely applied to the maximal cliques problem[83]. These methods significantly reduce the classical complexity compared with explicitly enumerating all possible generator groups in matrix A .

In genetic algorithm, the initial individual population is randomly generated, where each individual represents a potential stabilizer generator group. According to Eq. (14), the fitness function is defined as the weighted sum of Pauli expectation values with high energy penalty for non-commuting terms $C_{ij} \neq 0$. Through iterative selection, crossover, and mutation operation over successive generations, the population rapidly converges towards the configuration corresponding to the lowest stabilizer-group energy.

Through the above procedure, we can identify the stabilizer generator group G^{op} which yields the lowest stabilizer-group energy, here we define $|G^{op}| = l$. When $l = N$, a unique lowest-energy stabilizer generator group is obtained.

However, this stabilizer generator group is not always complete. In cases where $l < N$, additional $N - l$ stabilizer generators must be appended to G^{op} such that a full set of independent stabilizer generators can be formed. For such cases, the number of possible stabilizer generator group combinations is given by $2^{N-l} \prod_{i=1}^{N-l} (2^i + 1)$ which denotes the lowest energy degeneracy.

Fortunately, it is not necessary to explicitly list all the possible stabilizer generator groups and compute group energies individually. Using the genetic algorithm, we construct the maximally commuting generator group

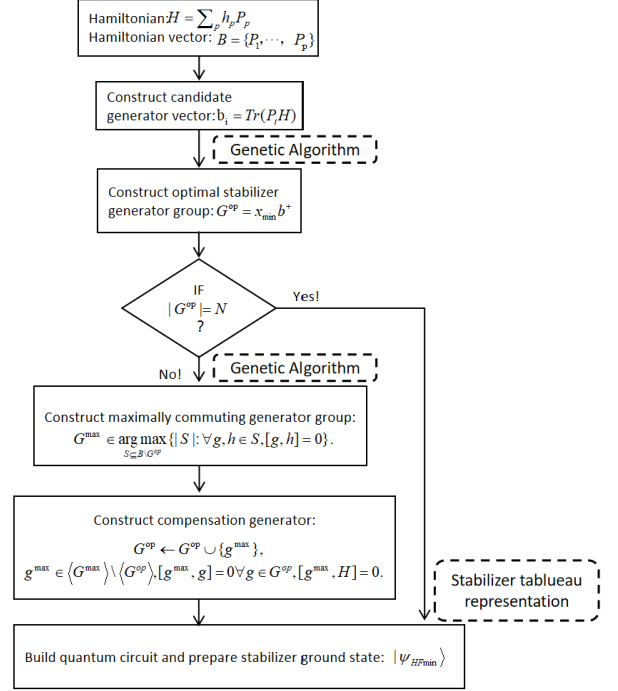


FIG. 1. The schematic plot for preparing optimal stabilizer ground state $|\psi_{OSGS \min}\rangle$

G^{\max} from the remaining generator set $B \setminus G^{op}$ which satisfies

$$G^{\max} \in \arg \max_{S \subseteq \mathcal{P}} \left\{ |S| : \forall g, h \in S, [g, h] = 0 \right\},$$

where $|G^{\max}| = f$. The order f determines the Hamiltonian lowest energy's degeneracy. When $f < N$, the lowest energy is 2^{N-f} -fold degenerate, with $f \geq l$. In this case, the optimal stabilizer ground state is not unique, leading to $2^{N-f} \prod_{i=1}^{N-f} (2^i + 1)$ distinct sets of stabilizer ground states that share the same highest-fidelity.

The strategy for inserting an additional stabilizer generator g^{\max} into G^{op} , in order to complete the stabilizer generator group and uniquely stabilize the optimal stabilizer ground state, must satisfy the following conditions:

$$G^{op} \leftarrow G^{op} \cup \{g^{\max}\};$$

$$\exists g^{\max} \in \langle G^{\max} \rangle \text{ s.t. } \begin{cases} [g^{\max}, g] = 0, & \forall g \in G^{op}, \\ g^{\max} \notin \langle G^{op} \rangle, \\ [g^{\max}, H] = 0. \end{cases} \quad (23)$$

We note that in the presence of lowest-energy degeneracy, the stabilizer generator group is not unique. All possible optimal generator groups stabilize the optimal stabilizer ground state. Accordingly, the problem separates into the following cases.

(1) Case $l = N$. In this case, the stabilizer ground state is uniquely determined by Eq. (14), and the identification of G^{op} is straightforward.

(2) Case $l = N$ and $f < N$. Here the lowest energy level is non-degenerate, but the stabilizer ground state remains degenerate. Consequently, multiple stabilizer generator groups yield the same stabilizer group energy with Eq. (14). The highest-fidelity generator group can then be selected by applying the filter function introduced in section III.

(3) Case $l < N$ and $f < N$. In this regime, both the stabilizer generator set and the maximal commuting group must be extended. By constructing G^{op} and G^{\max} , several distinct combinations of stabilizer generators may arise, each stabilizing a different stabilizer ground state.

The overall procedure for obtaining the optimal stabilizer ground state is summarized in Fig. 1. This constitutes a general framework for stabilizer-based ground-state preparation and may have broad applications in quantum computation and quantum information, such as in Lattice Schwinger model simulation for high energy physics quantum simulation [84, 85]. Another natural application arises in Ising model-type Hamiltonians: when the transverse-field term is absent, the stabilizer ground state is Hamiltonian's ground state. In such cases, the high-efficiency preparation achievable within our method substantially reduces the quantum-resource consumption.

V. APPLICATION TO QUANTUM SIMULATION

V.1. The measurement-based imaginary time evolution method

Let us briefly review how MITE algorithm works. The method can be understood as implementing imaginary-time evolution through a sequence of weak measurements. When the imaginary time $\tau \rightarrow \infty$, the imaginary-time evolution (ITE) sequence forces initial state evolve towards Hamiltonian's ground state, i.e.,

$$\lim_{\tau \rightarrow \infty} e^{-H\tau} |\psi_{\text{in}}\rangle = |E_0\rangle, \quad (24)$$

where $|\psi_{\text{in}}\rangle$ is an arbitrary initial state that can be written as the superposition of energy eigenstates as

$$|\psi_{\text{in}}\rangle = \sum_n A_n |E_n\rangle. \quad (25)$$

$|E_0\rangle$ is the ground state for Hamiltonian H .

In the MITE algorithm, the ITE scheme is implemented through a random sequence of weak measurements.

Those two weak measurement operators act as

$$M_0 = \sum_n \frac{1}{\sqrt{2}} (\cos \epsilon E_n - \sin \epsilon E_n) |E_n\rangle \langle E_n| \quad (26)$$

$$M_1 = \sum_n \frac{1}{\sqrt{2}} (\cos \epsilon E_n + \sin \epsilon E_n) |E_n\rangle \langle E_n| \quad (27)$$

which satisfy $M_0^\dagger M_0 + M_1^\dagger M_1 = I$. Weak measurement operators modify the amplitude distribution of the input state. As the number of measurement increases, the resulting amplitude distribution gradually approaches a Gaussian profile. This stochastic process effectively implements an imaginary-time filtering on the energy eigenbasis.

Unfortunately the random weak-measurement sequence does not always drive the state towards the ground state. After several measurement operations, the accumulated measurement outcomes allow us to estimate the effective energy distribution of the evolving state. Once the estimated energy exceeds the energy threshold E_{th} , a unitary correction operator U_c is applied to the system to reset the weak-measurement sequence. This feedback-based mechanism effectively implements an energy-filtering process: by repeatedly applying weak measurements and resetting the evolution whenever the amplitude function drift to the higher energy side, the algorithm ensures convergence toward the ground state from arbitrary initial state.

Let us analyze the quantum resource overhead of MITE and discuss how to optimize the algorithm. For an arbitrary initial state, the complexity for MITE scales polynomially with the system size, indicating a potential quantum advantage. The dominate quantum resource consumption in MITE arises from the repeated weak-measurement sequences. Each weak-measurement operation requires an ancillary qubit. A random initial state necessitates a long weak-measurement sequence to effectively suppress excited-state amplitude, thereby increasing the overall quantum resource cost.

V.2. Using optimal stabilizer ground state

The goal of the stabilizer-based optimal ground-state initialization is to accelerate the MITE scheme by preparing an optimized initial state using stabilizer formalism. This procedure is illustrated in Fig. 1. In other words, we can first prepare the optimal stabilizer ground state, which has the largest overlap with the true ground state. Then, by using the optimal stabilizer ground state $|\psi_{OSGS \min}\rangle$ as the input of the ITE scheme, the algorithm converges substantially faster.

This procedure can be justified as follows. The optimal stabilizer ground state attains the lowest stabilizer-group energy

$$E_{\min}^S = \langle \psi_{OSGS \min} | H | \psi_{OSGS \min} \rangle, \quad (28)$$

As shown in Eq. (14), E_{\min}^S is the weighted sum of the contributing Pauli terms determined by G^{op} .

We can expand $|\psi_{OSGS \min}\rangle$ in the eigenbasis of H

$$|\psi_{OSGS \min}\rangle = \sum_m A_m |E_m\rangle, \quad (29)$$

where $A_m = \langle \psi_{OSGS \min} | E_m \rangle$ denotes the overlap amplitude of $|\psi_{OSGS \min}\rangle$ projected onto the eigenstate $|E_m\rangle$

of Hamiltonian H .

According to Eq. (28), we will have

$$\langle \psi_{OSGS \min} | H | \psi_{OSGS \min} \rangle = \sum_m |A_m|^2 E_m, \quad (30)$$

$\sum_m |A_m|^2 = 1$. Since $|\psi_{OSGS \min}\rangle$ minimizes the stabilizer energy, its overlap with the true ground state is maximized, i.e., $|A_0|^2$ takes the largest value among all the amplitude A_m . The remaining amplitudes $A_{m>0}$ are distributed over excited states without any specific structure.

The speedup of MITE resulting from using $|\psi_{OSGS \min}\rangle$ as the initial state can be analyzed as follows. In the MITE algorithm, the weak measurement operators M_0 and M_1 adjust the amplitude associated with each energy eigenstate. In the energy eigenbasis, the effect of weak measurement sequence effect can be expressed as

$$M_0^{k_0} M_1^{k_1} = \sum_m \cos^{k_0}(\epsilon E_m + \frac{\pi}{4}) \sin^{k_1}(\epsilon E_m + \frac{\pi}{4}) |E_m\rangle \langle E_m|. \quad (31)$$

By choosing $\epsilon E_n \in [-\frac{\pi}{4}, \frac{\pi}{4}]$, the amplitude function exhibits a Gaussian-like envelop over energy spectrum.

When $|\psi_{OSGS \min}\rangle$ is used as the initial state, the resulting amplitudes take the form

$$M_0^{k_0} M_1^{k_1} |\psi_{OSGS \min}\rangle = \sum_m A(\epsilon E_m) |E_m\rangle, \quad (32)$$

$$A(\epsilon E_m) = A_m \cos^{k_0}(\epsilon E_m + \frac{\pi}{4}) \sin^{k_1}(\epsilon E_m + \frac{\pi}{4}), \quad (33)$$

where $A(\epsilon E_m)$ denotes the normalized energy-resolved amplitude after the weak-measurement sequence which satisfies $\sum_m |A(\epsilon E_m)|^2 = 1$. And $|A(\epsilon E_m)|^2$ represents the weight of energy $|E_m\rangle$ in weak-measurement step. For the optimal stabilizer ground state $|\psi_{OSGS \min}\rangle$, the ground state amplitude satisfies

$$|A_0|^2 = \max_m |A_m|^2. \quad (34)$$

Because this initial state overlap A_0 is larger than random case, the weak-measurement sequence needed for convergence is significantly reduced.

Another advantage is that the OSGS-based MITE scheme does not require explicit energy-spectrum to determine the threshold. Although the lowest stabilizer-group energy E_{\min}^S may be higher than conventional threshold $E_{th} = \frac{E_0 + E_1}{2}$, the enhanced initial overlap ensures that the MITE dynamics convergence toward the true ground state $|E_0\rangle$. Although E_{\min}^S will be larger than E_{th} in some case, $|\psi_{OSGS \min}\rangle$ can compensate the shortage of energy threshold and the scheme will converge to the ground state $|E_0\rangle$ as well. The numerical simulation result of average fidelity in Sec. (V.4) can also demonstrate that. Moreover, the OSGS-based MITE can be served as an efficient tool for ground-state energy estimation which can be another potential advantage. Once OSGS-based MITE evolved to the ground state through MITE process, the ground-state energy can be directly obtained via $E_0 = \langle E_0 | H | E_0 \rangle$.

V.3. Complexity analysis and convergence error

The overall complexity of the OSGS-based MITE consists of two parts: (i) the preparation of the optimal stabilizer ground state, and (ii) the optimized MITE scheme. We discuss the classical computational cost and quantum circuit depth associated with each step.

The candidate generator set \mathbf{b} contains 2^{2N+1} Pauli coefficients arising from the Hamiltonian decomposition. In \mathbf{b} , only those entries whose Pauli operators appear in the Hamiltonian will be non-zero. Let p denotes the number of non-zero Pauli terms in the Hamiltonian. Then the construction of \mathbf{b} costs $O(p)$. The matrix A encodes all possible stabilizer generators candidates for N -qubit system. It can be the a general reference matrix for N qubit system. Although the stabilizer group contains 4^N Pauli operators, the independent stabilizer generators are at most N . And the computation of $A^\dagger \mathbf{b}$ involves those pairs where both the Hamiltonian terms and the corresponding stabilizer generator are non-zero. Since each stabilizer generator group contains at most $O(N)$ non-zero Pauli components, the total classical cost is $O(Np)$.

Due to the Gottesman-Knill theorem, stabilizer state preparation procedure can be efficiently simulated with classical computation[8]. The original simulation algorithm requires $O(N^3)$ time for simulating N -qubit stabilizer circuit. Then by employing more efficient update rules, the time consumption was improved to $O(N^2)$ [48]. Stabilizer tableau representation requires $N(2N+1)$ bits to specify the stabilizer group classically. Regarding quantum circuit depth complexity, any unitary stabilizer circuit can be implemented with $O(N^2/\log N)$ gates in the worst case [48, 86, 87].

In the case where $[g_i, H] = 0$ for all generators g_i of the optimal stabilizer generator group G^{op} , the stabilizer state prepared via the stabilizer tableau method corresponds to the ground state of Hamiltonian H . Under such conditions, the quantum circuit for preparing this ground state requires $O(N^2/\log N)$ gates.

In contrast, for the other cases, MITE scheme becomes necessary for deterministic ground state preparation. This procedure generally requires a polynomial number of quantum gates for a N -qubit system. In such scheme, circuit depth depends critically on several factors: the initial fidelity $\mathcal{F}(|\psi_s\rangle, |E_0\rangle)$, $\mathcal{F}(|\psi_s\rangle, |E_1\rangle)$, and the relative energy factor $\epsilon E_0 + \pi/4$. We will show more demonstration detail in the appendix C.

For the algorithm error analysis, we quantify the convergence error with $\mathcal{E} = 1 - \mathcal{F}$, where \mathcal{F} is the fidelity between the evolved state and the true ground state. When quantum state evolves for a sufficiently large number of iterations, the system converges to the ground state with an error bounded by \mathcal{E} . The convergence error after k iterations is given as

$$\mathcal{E} \approx \frac{\mathcal{F}(|\psi_s\rangle, |E_1\rangle)}{\mathcal{F}(|\psi_s\rangle, |E_0\rangle)} e^{2k\epsilon^2(E_0 - E_1)(E_0 + E_1 - 2E_{th})}. \quad (35)$$

Eq. (35) provides the primary constraint of our quantum

algorithm. The Error \mathcal{E} is determined by the initial fidelity ratio, the number of weak measurements, and the energy spectral properties of Hamiltonian. By preparing the stabilizer ground state firstly, the initial fidelity ratio ensures the error is critically suppressed and consequently reduces the required number of weak measurements k . This mechanism explains why initializing the algorithm with a stabilizer ground state improves the efficiency of MITE scheme. More details will be given in Appendix D.

V.4. Numerical simulation

We evaluate the performance of our OSGS-based MITE scheme using the transverse-field Ising model (TFIM), which serves as a natural platform for studying quantum phase transitions [88]. When the transverse field is removed, the model reduces to the classical Ising Hamiltonian, for which stabilizer ground states can be prepared exactly. In such cases, our OSGS-based MITE scheme can obtain the exact ground state using only Clifford gates and Pauli measurements, demonstrating a clear advantage in circuit-depth efficiency compared with specialized Ising-machine solvers. As reported in Refs.[48, 89], Clifford-based approaches can achieve circuit-depth scaling as low as $N^2/\log N$, aligning with the resource efficiency of our method.

We consider an $L = 5$ qubit transverse Ising model, whose Hamiltonian is written as

$$H = \sum_{i=1}^{L-1} Z_i Z_{i+1} + \lambda \sum_{j=1}^L X_j. \quad (36)$$

As we discussed earlier, the choice of optimal stabilizer generator group G^{op} depends on the value of λ , since the lowest stabilizer group energy is determined by the weighted contributions of the Pauli terms that appear in Hamiltonian H . We will analyze G^{op} within different parameter regimes of λ .

When $\lambda = 0$, transverse-field Ising model reduces to the standard Ising model. In such case, the ground state can be obtained directly within the stabilizer-state preparation procedure through an appropriate update of the stabilizer tableau representation.

For $\lambda \neq 0$, the optimal stabilizer generator group G^{op} is selected according to Eq. (14). This criterion yields two candidate optimal stabilizer generator sets: (i) $G^{\max} = \{-X_1, -X_2, -X_3, -X_4, -X_5\}$, contributing a stabilizer energy of -5λ ; and (ii) $\{-Z_1 Z_2, -Z_2 Z_3, -Z_3 Z_4, -Z_4 Z_5\}$ which contributes -4 . In such case, the phases of the generator are chosen such that the stabilizer group energy is minimized.

If $\lambda < 0.8$, the optimal generator group is determined to be $G^{op} = \{-Z_1 Z_2, -Z_2 Z_3, -Z_3 Z_4, -Z_4 Z_5\}$, which yields the minimal stabilizer group energy $E_{\min}^S = -4$. In this regime, the sub-Hamiltonian associated with the transverse field is $H_{\text{sub}} = \lambda \sum_{j=1}^5 X_j$. In this case, G^{op}

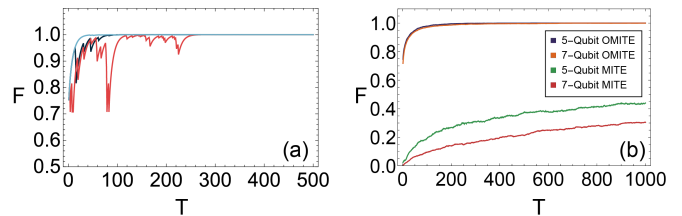


FIG. 2. Performance of the OSGS-based MITE scheme applied to the transverse-field Ising model at $\lambda = 0.6$. (a) Solid curves (in three different colors) show representative evolution trajectories of the random MITE procedure, while the black dashed curve denotes the fidelity averaged over 1000 independent random MITE trials. (b) Comparison of the averaged fidelity over 1000 turns for the MITE with and without stabilizer ground state preparation for 5-qubit and 7-qubit cases.

does not form a complete set of N independent stabilizer generators, an additional generator must be included to ensure full stabilization over 5-qubits' Hilbert space. A natural and optimal choice is $g = -X_1 X_2 X_3 X_4 X_5$. The reason is twofold. The first reason is that the generator which produced by the multiplication of G^{\max} and restricted to be the sub-Hamiltonian H_{sub} ; and it satisfies $[g, H] = 0$ which is the core criterion of filter function Eq. (17), thereby preserving the highest fidelity condition. The numerical results for $\lambda = 0.6$ are shown in Fig. 2(a). Each solid line represents a different random weak-measurement trajectory of the OSGS-based MITE protocol. The minimal fidelity observed across all trajectories is 0.707, which corresponds precisely to the fidelity between the chosen stabilizer ground state and the true ground state.

When $\lambda \geq 0.8$, then the optimal generator group is $G^{op} = \{-X_1, -X_2, -X_3, -X_4, -X_5\}$, which forms a complete and independent generator set. The stabilizer ground state prepared from this group is used as the initial state for MITE procedure, this initial state will converge to the true ground state similar to the trajectories that shown in Fig. 2(a).

Figure 2(b) compares the performance of the MITE's algorithm with and without stabilizer ground state preparation for 5-qubit and 7-qubit Ising model cases. The inclusion of the stabilizer ground state as the initial state leads to a substantially faster convergence of the average fidelity compared with the original MITE scheme. By comparing different quantum system scales (a 5-qubit system and a 7-qubit system), we find that, when assisted by the stabilizer ground state, the convergence speed of the MITE algorithm remains nearly unchanged as the system size increases. The algorithm's performance contrasts sharply with the standard MITE procedure, for which the convergence rate degrades significantly with increasing system size.

VI. CONCLUSIONS

In this work, we propose a hybrid method for efficient ground state preparation. The basic idea is to first prepare a optimal stabilizer ground state which is closest to the true ground state. Within the stabilizer formalism, the task of preparing the optimal stabilizer ground state can be reformulated as the problem of identifying the corresponding independent stabilizer generator group. This problem can be addressed using two distinct strategies. The selection of optimal stabilizer generators can be achieved using either a magic witness-based criterion or a genetic algorithm-based search, which guarantees the generality and applicability of the method across different Hamiltonians. In cases where the stabilizer generators directly derived from the Hamiltonian are not sufficient to form a complete and independent stabilizer generator set, additional generators are selected from the maximally commuting group G^{\max} using same genetic-algorithm strategy. Leveraging the stabilizer tableaux representation, the resulting stabilizer ground state can be prepared by a quantum circuit with constant depth.

The highest fidelity and lowest energy property makes stabilizer ground state an excellent candidate for ground-state preparation. We demonstrate its application by implementing the optimal stabilizer ground state into measurement-based imaginary time evolution (MITE) procedure. Numerical simulation results show that initializing MITE with the optimal stabilizer ground state can significantly accelerate convergence toward the true ground state.

The advantage of the proposed method are twofold. First, by incorporating classical computation, this hybrid approach significantly improves the overall algorithmic efficiency. Second, it provides a general framework for ground-state search that does not rely on prior knowledge of system's energy spectrum. The stabilizer ground-state energy serves as a potential energy threshold for MITE scheme, determining whether the evolving state need to be corrected. Several avenues exist for further enhancement of this method. Quantum algorithms such as quantum annealing may offer alternative approaches for constructing optimal stabilizer generator sets in Eq. (23). What's more, the efficiency and the scalability of the RoM criterion remain important open questions for future study.

ACKNOWLEDGMENTS

This research is supported by the Natural Science Foundation of Zhejiang Province under Grant No. LQN26A050002. T.B. is supported by the SMEC Scientific Research Innovation Project (2023ZKZD55); the Science and Technology Commission of Shanghai Municipality (22ZR1444600); the NYU Shanghai Boost Fund; the China Foreign Experts Program (G2021013002L); the NYU-ECNU Institute of Physics at NYU Shanghai;

the NYU Shanghai Major-Grants Seed Fund; and Tamkeen under the NYU Abu Dhabi Research Institute grant CG008.

DATA AVAILABILITY

No data were created or analyzed in this study.

APPENDIX A: PROOF OF EQ. (14)

Here we show that the stabilizer group energy can be evaluated using Eq. (11). The matrix A^\dagger encodes the stabilizer group G_m that are feasible for an arbitrary N qubit system. From each stabilizer group $G_m = \{g_{m1}, \dots, g_{m2^N}\}$, we may select N mutually commuting and independent generators to form an independent stabilizer generator set

$$\mathcal{G}_m^S = \{\tilde{g}_1, \tilde{g}_2, \dots, \tilde{g}_N\} \subset G_m, \quad |\mathcal{G}_m^S| = N. \quad (\text{A1})$$

The stabilizer group is then given by the group generated by these generators,

$$G_m = \langle \mathcal{G}_m^S \rangle. \quad (\text{A2})$$

The corresponding pure stabilizer state $|\psi_s\rangle$ has density matrix as

$$\rho_s = |\psi_s\rangle\langle\psi_s| = \frac{1}{2^N} \prod_{j=1}^N (I^{\otimes N} + \tilde{g}_j). \quad (\text{A3})$$

The factor $1/2^N$ ensures normalization of the projector onto the stabilizer subspace.

The stabilizer group energy is the expectation value of the Hamiltonian with respect to $|\psi_s\rangle$:

$$\begin{aligned} \langle H \rangle_s &= \text{Tr}(H\rho_s) \\ &= \frac{1}{2^N} \text{Tr} \left(\sum_p h_p P_p \prod_{j=1}^N (I^{\otimes N} + \tilde{g}_j) \right) \\ &= \frac{1}{2^N} \sum_p h_p \text{Tr} \left[P_p \left(I^{\otimes N} + \sum_{i=1}^{2^N} g_{mi} \right) \right]. \end{aligned} \quad (\text{A4})$$

The trace yields non-zero result only when $P_p = g_{mi}$ for $g_{mi} \in G_m$, in which case

$$\text{Tr}(P_p g_{mi}) = 2^N \text{sgn}(g_{mp}). \quad (\text{A5})$$

Therefore, the stabilizer group energy reduces to

$$\langle H \rangle_s = \sum_p h_p \text{sgn}(g_{mp}), \quad (\text{A6})$$

which shows the same result as Eq. (11).

APPENDIX B: SELECTION STRATEGY FOR OPTIMAL STABILIZER GENERATOR GROUP

As stated in the main text, the strategy for selecting the optimal stabilizer generator group is two-step procedure. In this appendix we explain why the stabilizer generator group may not be unique and then prove strategy's feasibility step by step.

By definition, a stabilizer ground state is the stabilizer state that attains the lowest Hamiltonian expectation value (see Eq. (14)). For an N -qubit system with a Hamiltonian containing p Pauli terms, the stabilizer generator group is selected from the Hamiltonian set \mathcal{S} . Constructing an independent stabilizer generator group requires at least N mutually commuting stabilizer generators, as implied by stabilizer formalism and the Gottesman-Knill framework. However, It is uncommon to find N mutually commuting generators within the \mathcal{S} whose weighted sum attains the minimal value. Consequently, when pursuing the minimal stabilizer energy E_{\min}^S , the set of contributing generator terms from B may contain less than N elements. This set is denoted as G_{com} in the main text. To complete the stabilizer generator group, some extra generators needs to be added into G_{com} .

The number of possible groups $G_{\min}^{(p)}$ in the group G_{\min} is

$$|G_{\min}| = 2^m \prod_{i=1}^m (2^i + 1), \quad m = N - |G_{\text{com}}|. \quad (\text{B1})$$

In the first step, we define a filter function and discard any generator group whose elements do not commute with Hamiltonian H . This restriction becomes essential in the subsequent fidelity calculation. We consider a generator group G_{\min} that includes the common subgroup G_{com} , i.e., $G_{\text{com}} \subseteq G_{\min}$. The group G_{\min} stabilize state $|\psi_s\rangle$. The corresponding independent stabilizer generator set of G_{\min} is defined as \mathcal{G}_{\min} . the fidelity between state $|\psi_s\rangle$ and Hamiltonian's ground state $|E_0\rangle$ is then written as

$$\begin{aligned} \mathcal{F}(|E_0\rangle, |\psi_s\rangle) &= \langle E_0 | \psi_s \rangle \langle \psi_s | E_0 \rangle \\ &= \left\langle E_0 \left| \prod_{j=1}^N \frac{I + \tilde{g}_j}{2} \right| E_0 \right\rangle, \end{aligned} \quad (\text{B2})$$

in which $\tilde{g}_j \in \mathcal{G}_{\min}$. The independent stabilizer generator group can be decomposed as

$$\mathcal{G}_{\min} = G_{\text{com}} \cup G_{\text{extra}}, \quad (\text{B3})$$

Where G_{com} 's element is extracted from the candidate generator set \mathbf{b} , and G_{extra} contains the additional generators.

Stabilizer generators in G_{com} do not commute with the Hamiltonian H . This is because the elements of G_{com} doesn't commute with each operators in B , while the

Hamiltonian H is a weighted sum of the operators in B . Equation (B2) can therefore be rewritten as

$$\mathcal{F}(|E_0\rangle, |\psi_s\rangle) = \left\langle E_0 \left| \prod_{i \in G_{\text{com}}} \frac{I + \tilde{g}_i}{2} \prod_{j \in G_{\text{extra}}} \frac{I + \tilde{g}_j}{2} \right| E_0 \right\rangle. \quad (\text{B4})$$

In this expression, the product of generators belonging to G_{com} is fixed because it is determined directly by the structure of the Hamiltonian. The degree of freedom lies in selecting the generators within G_{extra} . To maximize the fidelity, choosing the generator \tilde{g}_j satisfying $[\tilde{g}_j, H] = 0$ is optimal. If the generator \tilde{g}_j commutes with the Hamiltonian H , then \tilde{g}_j and H same a common eigenbasis, which implies

$$\tilde{g}_j |E_0\rangle = \pm 1 |E_0\rangle. \quad (\text{B5})$$

Since Pauli strings is Hermitian and squares to the identity, each generator \tilde{g}_i has eigenvalues restricted to ± 1 . Substituting Eq. (B5) into Eq. (B4), the fidelity becomes

$$\mathcal{F}(|E_0\rangle, |\psi_s\rangle) = \begin{cases} \langle E_0 | \prod_{i \in G_{\text{com}}} \frac{I + \tilde{g}_i}{2} |E_0\rangle, & \forall \tilde{g}_j |E_0\rangle = |E_0\rangle \\ 0, & \exists \tilde{g}_j |E_0\rangle = -|E_0\rangle \end{cases} \quad (\text{B6})$$

Such that in the first step-testing whether each candidate generator commutes with the Hamiltonian H -we discard all generator groups whose elements lead to a fidelity reduction. However, this procedure alone cannot remove the groups that yield a lowest fidelity approach to 0. This limitation arises because stabilizer generators are allowed to appear with phases ± 1 , consequently, additional filtering is required to control generator's phase and eliminate the near-zero fidelity result.

In the first step, we construct \mathcal{G}_{\min} by considering the contribution of Pauli string in G_{com} . However, if this step does not converge to a unique stabilizer generator group, we must further incorporate Pauli strings $B \setminus C_{\text{com}}$ to constrain the generator's phase(i.e., the ± 1 ambiguity).

In the second step, we define a sub-Hamiltonian by removing all the Pauli terms contained in C_{com} . We then evaluate the candidate generator set using Eq. (10) and search for the corresponding generator group $\mathcal{G}_{\min}^{\text{sub}}$ that takes the lowest stabilizer group energy E_{\min}^S as expressed in Eq. (14). This procedure is same as we did in determining G_{\min} , the aim is to identify the stabilizer ground state associated with the reduced Hamiltonian H_{sub} .

$\mathcal{G}_{\min}^{\text{sub}}$ contains the stabilizer information determined by the sub-Hamiltonian H_{sub} . By evaluating the filter function $\xi(\mathcal{G}_{\min}^{\text{sub}}, H)$ and selecting the generators that lie in the intersection of \mathcal{G}_{\min} and $\mathcal{G}_{\min}^{\text{sub}}$, we obtain the optimized generator set \mathcal{G}^{op} . Conceptually, step two determines the generator's phase(± 1) of each stabilizer generator by enforcing consistency with all Pauli terms in H_{sub} . This phase-refinement process yields the final optimized generator group \mathcal{G}^{op} .

APPENDIX C: COMPLEXITY ANALYSIS OR THE ALGORITHM

To analyze the computational complexity of the algorithm, we begin by considering the stabilizer ground state that attains the lowest fidelity with the true ground state. This represents the worst-case scenario, in which the algorithm requires the largest amount of quantum resources. The system Hamiltonian is assumed to take the form

$$H = \sum_{p=1}^{2N} h_p P_p, \quad (\text{C1})$$

where all the weight factors are identical $h_p = C$. We further assume that $|G^{op}| = N$ with $G^{op} \subset B$, and that in this worst-case setting the G^{op} has two possible configurations, both yielding the lowest achievable fidelity with the true ground state.

To establish the relation between the measurement times k_0 and the convergence in energy, we analyze the action of applying measurement operator M_0 repeatedly. After performing k rounds of the M_0 measurement, the post-measurement state is driven toward the true ground state $|E_0\rangle$. With the assumption that the projection effect of M_0 only changes the normalized amplitude associated with $|E_0\rangle$, such that the fidelity satisfies

$$\begin{aligned} \mathcal{F}(M_0^k |\psi_s\rangle, |E_0\rangle) &= \langle \psi_s | (M_0^\dagger)^k | E_0 \rangle \langle E_0 | (M_0)^k | \psi_s \rangle \\ &= \cos^{2k}(\epsilon E_0 + \pi/4) \mathcal{F}(|\psi_s\rangle, |E_0\rangle). \end{aligned} \quad (\text{C2})$$

This expression characterizes the exponential amplification of the ground-state component induced by iterative measurement and forms the basis for estimating the measurement complexity k_0 required to reach the target ground state within a specified energy precision. By solve Eq. (C2), we obtain the convergence condition

$$k = \frac{\ln \mathcal{F}(|\psi_s\rangle, |E_0\rangle)}{2 \ln(1/\cos(\epsilon E_0 + \pi/4))}. \quad (\text{C3})$$

Eq. (C3) quantifies the quantum resource requirement for the shortest successful convergence process under the idealized assumption that the MITE protocol performs only the M_0 weak measurement at each iteration. In this case, fidelity grows monotonically, and the number of iterations required to reach the true ground state can be directly computed from the amplification factor associated with M_0 . However, in reality the weak measurements M_0 and M_1 occur randomly.

As shown in Eq. (33), the action of M_0 accumulates the amplitude weight in the low energy side, whereas M_1 have the opposite effect. Consequently, the actual number of measurements required to achieve a given precision generally exceeds the ideal bound in Eq. (C3), and the convergence behavior must be understood as the result of a probabilistic sequence of competing amplitude-update events.

To ensure that the algorithm converges to the ground state deterministically, we introduce the energy threshold together with quantum state reset mechanism. The energy threshold is chosen as the energy expectation value E_{\min}^S , i.e., the energy of stabilizer ground state. The quantum state reset condition can be expressed as

$$\langle E_0 | M_1 M_0^{k'} | E_0 \rangle \geq \langle E_1 | M_1 M_0^{k'} | E_1 \rangle. \quad (\text{C4})$$

This state reset mechanism requires that the amplitude of ground state component is always dominant compared to the first excited energy state. Eq. (C4) inequality provides the amplitude criterion under which the undesired amplification of the first excited state remains bounded. Once the inequality is violated, quantum state will be reset to the stabilizer ground state. Physically, this rule captures the intuition that the effect of one M_1 measurement must be compensated by sufficiently large k times of M_0 measurements to retrieve the amplitude dominance of the ground state.

By simplifying Eq. (C4) using the amplitude factors associated with M_0 and M_1 , we obtain the condition that M_0 measurement times k must satisfy

$$k' \geq \frac{\ln[\cos(\epsilon E_1 - \pi/4)] - \ln[\cos(\epsilon E_0 - \pi/4)]}{\ln[\cos(\epsilon E_0 + \pi/4)] - \ln[\cos(\epsilon E_1 + \pi/4)]}. \quad (\text{C5})$$

Whenever k' fails to satisfy this inequality, system will be reset. In particular, any weak-measurement sequence initiated by an M_1 event—such as M_1 , $M_1 M_0$, $M_1 M_0^2$ —is discarded unless it is compensated by a sufficiently large number of subsequent M_0 measurements. The energy threshold and reset mechanism ensures that quantum state converges deterministically toward the ground state.

We define the average failure length as

$$\begin{aligned} T_{\text{fail}} &= \sum_{k_a=0}^{k'} k_a \cdot p_{1|k_a-1} \cdot p_{k_a-1} \\ &= \sum_{k_a=1}^{k'} k_a \cdot [\cos^{2k_a-2}(\epsilon E_0 + \pi/4) \mathcal{F}(|\psi_s\rangle, |E_0\rangle) \\ &\quad + \cos^{2k_a-2}(\epsilon E_1 + \pi/4) \mathcal{F}(|\psi_s\rangle, |E_1\rangle) \\ &\quad - \cos^{2k_a}(\epsilon E_0 + \pi/4) \mathcal{F}(|\psi_s\rangle, |E_0\rangle) \\ &\quad - \cos^{2k_a}(\epsilon E_1 + \pi/4) \mathcal{F}(|\psi_s\rangle, |E_1\rangle)], \end{aligned} \quad (\text{C6})$$

when measurement times increase, the weak-measurement process progressively suppress the amplitudes associated with higher-energy eigenstates. Consequently, the dominant contributions to the failure possibility arise from the ground state $|E_0\rangle$ and the first excited state $|E_1\rangle$. Therefore, for evaluating T_{fail} , it is sufficient to maintain only the fidelity terms involving E_0 and E_1 , as higher excited states' contribution is negligible.

To further simplify Eq. (C6) and Eq. (C5), we analyze the extreme and most resource-consuming scenario

in which the energy gap between ground state and first excited state approaches zero, i.e.

$$E_1 - E_0 \rightarrow 0^+. \quad (\text{C7})$$

In this limit, Eq. (C5) will be simplified as

$$\lim_{E_1 - E_0 \rightarrow 0^+} \frac{\ln(\cos(\epsilon E_1 - \pi/4)) - \ln(\cos(\epsilon E_0 - \pi/4))}{\ln(\cos(\epsilon E_0 + \pi/4)) - \ln(\cos(\epsilon E_1 + \pi/4))} = 1/(\epsilon E_0 + \pi/4)^2, \quad (\text{C8})$$

where $\epsilon E_0 + \pi/4 \neq 0$. Thus, in the worst scenario, the reset energy threshold requires an average of $M = \lceil \frac{1}{(\epsilon E_0 + \pi/4)^2} \rceil$. With the above approximation, the total number of measurements required for a successful procedure cycle can be written as

$$\begin{aligned} T_{tot} &= T_{\text{fail}} + k \\ &= (\mathcal{F}(|\psi_s\rangle, |E_0\rangle) + \mathcal{F}(|\psi_s\rangle, |E_1\rangle)) \cdot \frac{1+q}{1-q} \\ &\quad \cdot [Mq^M - (M+1)q^{M-1} + \frac{1}{q}] - \frac{\ln(\mathcal{F}(|\psi_s\rangle, |E_0\rangle))}{2 \ln q}, \end{aligned} \quad (\text{C9})$$

where $q = \cos(\epsilon E_0 + \pi/4)$.

Eq. (C9) provides the total weak-measurement complexity of the MITE protocol in the most challenging case. The total resource scaling is polynomial in the system size and depends only on the inverse energy scale and initial fidelity. This result highlights the intrinsic quantum advantage of the MITE algorithm compared with classical methods whose complexity grows exponentially.

APPENDIX D: ALGORITHM'S ERROR ESTIMATION

To access the algorithm's error, we consider the worst scenario in which the amplitude peak satisfies

$$x_{k_0 k_1}^{\max} = \epsilon E_{th} \quad (\text{D1})$$

Let the algorithm's initial state be $|\psi_s\rangle$. After implementing $k_0 + k_1$ times of weak measurements, the resulting state can be expressed as

$$M_0^{k_0} M_1^{k_1} |\psi_s\rangle = \sum_n A(\epsilon E_n) \langle E_n | \psi_s \rangle |E_n\rangle, \quad (\text{D2})$$

where $A(\epsilon E_n)$ represents the accumulated amplitude factor associated with energy level E_n .

With the assumption of sufficient weak measurements ($\epsilon \ll 1$) and sufficient large total measurement times $K = k_0 + k_1$, the amplitude function can be approximated by a Gaussian distribution. Specifically, Amplitude function $A(x)$ can be expressed as

$$A(x) \propto e^{-K(x - x_{k_0 k_1}^{\max})^2} = e^{-K(\epsilon E_n - \epsilon E_{th})^2}, \quad (\text{D3})$$

where $x_{k_0 k_1}^{\max}$ shows the Gaussian shape's peak position. It is determined by the relative proportions of measurement times k_0 and k_1 .

To quantify the performance of weak-measurement process, We evaluate the normalized fidelity between the post-measurement state and true ground state after $K = k_0 + k_1$ times of weak measurements

$$\begin{aligned} \mathcal{F} &= \frac{|A(\epsilon E_0) \langle E_0 | \psi_s \rangle|^2}{\sum_n |A(\epsilon E_n) \langle E_n | \psi_s \rangle|^2} \\ &= \frac{1}{1 + \sum_n \frac{|A(\epsilon E_n) \langle E_n | \psi_s \rangle|^2}{|A(\epsilon E_0) \langle E_0 | \psi_s \rangle|^2}}. \end{aligned} \quad (\text{D4})$$

Since the amplitude function $A(\epsilon E_n)$ decays rapidly for $E_n > E_0$ when measurement time increase, the contribution from higher-energy states becomes negligible. For a approximation, we can only consider lowest and first excited energy amplitude's contribution which is shown as

$$\begin{aligned} \mathcal{F} &\approx \frac{1}{1 + \frac{|A(\epsilon E_1) \langle E_1 | \psi_s \rangle|^2}{|A(\epsilon E_0) \langle E_0 | \psi_s \rangle|^2}} \\ &\approx 1 - \frac{|A(\epsilon E_1) \langle E_1 | \psi_s \rangle|^2}{|A(\epsilon E_0) \langle E_0 | \psi_s \rangle|^2}. \end{aligned} \quad (\text{D5})$$

This approximation becomes increasingly accurate for large K , where the weak-measurement process strongly suppresses the excited-state population, yielding a fidelity that approaches unity.

The algorithmic error is defined as

$$\mathcal{E} = 1 - \mathcal{F}. \quad (\text{D6})$$

Substituting Eq. (D5) into the above definition yields

$$\mathcal{E} \approx \frac{\mathcal{F}(|\psi_s\rangle, |E_1\rangle)}{\mathcal{F}(|\psi_s\rangle, |E_0\rangle)} e^{2K\epsilon^2(E_0 - E_1)(E_0 + E_1 - 2E_{th})}. \quad (\text{D7})$$

This expression shows that the algorithmic error is governed by three factors: the initial fidelity ratio $\mathcal{F}(|\psi_s\rangle, |E_1\rangle)/\mathcal{F}(|\psi_s\rangle, |E_0\rangle)$, measurement times K and the relative position of energy threshold respect to the first two eigenenergies. When we prepare the stabilizer ground state, the initial overlap with the excited states is typically suppressed, leading to

$$\frac{\mathcal{F}(|\psi_s\rangle, |E_1\rangle)}{\mathcal{F}(|\psi_s\rangle, |E_0\rangle)} \rightarrow 0. \quad (\text{D8})$$

In this regime, the error \mathcal{E} naturally vanishes regardless of the exact value of K , demonstrating the robustness of the OSGS-based MITE scheme.

-
- [1] L. Gyongyosi and S. Imre, A survey on quantum computing technology, *Computer Science Review* **31**, 51 (2019).
- [2] T. D. Ladd, F. Jelezko, R. Laflamme, Y. Nakamura, C. Monroe, and J. L. O'Brien, Quantum computers, *nature* **464**, 45 (2010).
- [3] A. Steane, Quantum computing, *Reports on Progress in Physics* **61**, 117 (1998).
- [4] C. P. Williams, *Explorations in quantum computing* (Springer Science & Business Media, 2010).
- [5] D. Bluvstein, S. J. Evered, A. A. Geim, S. H. Li, H. Zhou, T. Manovitz, S. Ebadi, M. Cain, M. Kalinowski, D. Hangleiter, *et al.*, Logical quantum processor based on reconfigurable atom arrays, *Nature* **626**, 58 (2024).
- [6] F. Arute, K. Arya, R. Babbush, D. Bacon, J. C. Bardin, R. Barends, R. Biswas, S. Boixo, F. G. Brandao, D. A. Buell, *et al.*, Quantum supremacy using a programmable superconducting processor, *Nature* **574**, 505 (2019).
- [7] I. M. Georgescu, S. Ashhab, and F. Nori, Quantum simulation, *Reviews of Modern Physics* **86**, 153 (2014).
- [8] M. A. Nielsen and I. L. Chuang, *Quantum computation and quantum information* (Cambridge university press, 2010).
- [9] I. Bloch, J. Dalibard, and W. Zwerger, Many-body physics with ultracold gases, *Reviews of modern physics* **80**, 885 (2008).
- [10] T. Byrnes and E. O. Ilo-Okeke, *Quantum atom optics: Theory and applications to quantum technology* (Cambridge university press, 2021).
- [11] A. J. Daley, I. Bloch, C. Kokail, S. Flannigan, N. Pearson, M. Troyer, and P. Zoller, Practical quantum advantage in quantum simulation, *Nature* **607**, 667 (2022).
- [12] I. N. Levine, D. H. Busch, and H. Shull, *Quantum chemistry*, Vol. 6 (Pearson Prentice Hall Upper Saddle River, NJ, 2009).
- [13] C. W. Bauer, Z. Davoudi, A. B. Balantekin, T. Bhattacharya, M. Carena, W. A. De Jong, P. Draper, A. El-Khadra, N. Gemelke, M. Hanada, *et al.*, Quantum simulation for high-energy physics, *PRX quantum* **4**, 027001 (2023).
- [14] B. Nachman, D. Provasoli, W. A. De Jong, and C. W. Bauer, Quantum algorithm for high energy physics simulations, *Physical review letters* **126**, 062001 (2021).
- [15] W. Hofstetter and T. Qin, Quantum simulation of strongly correlated condensed matter systems, *Journal of Physics B: Atomic, Molecular and Optical Physics* **51**, 082001 (2018).
- [16] T. Byrnes, P. Recher, N. Y. Kim, S. Utsunomiya, and Y. Yamamoto, Quantum simulator for the hubbard model with long-range coulomb interactions using surface acoustic waves, *Physical review letters* **99**, 016405 (2007).
- [17] R. Dovesi, A. Erba, R. Orlando, C. M. Zicovich-Wilson, B. Civalleri, L. Maschio, M. Rérat, S. Casassa, J. Baima, S. Salustro, *et al.*, Quantum-mechanical condensed matter simulations with crystal, *Wiley Interdisciplinary Reviews: Computational Molecular Science* **8**, e1360 (2018).
- [18] B. Fauseweh, Quantum many-body simulations on digital quantum computers: State-of-the-art and future challenges, *Nature Communications* **15**, 2123 (2024).
- [19] H. Tasaki, *Physics and mathematics of quantum many-body systems*, Vol. 66 (Springer, 2020).
- [20] G. Vidal, Efficient simulation of one-dimensional quantum many-body systems, *Physical review letters* **93**, 040502 (2004).
- [21] J. Eisert, M. Friesdorf, and C. Gogolin, Quantum many-body systems out of equilibrium, *Nature Physics* **11**, 124 (2015).
- [22] S. Lloyd, Universal quantum simulators, *Science* **273**, 1073 (1996).
- [23] D. S. Abrams and S. Lloyd, Simulation of many-body fermi systems on a universal quantum computer, *Physical Review Letters* **79**, 2586 (1997).
- [24] H. Wang, S. Ashhab, and F. Nori, Efficient quantum algorithm for preparing molecular-system-like states on a quantum computer, *Physical Review A—Atomic, Molecular, and Optical Physics* **79**, 042335 (2009).
- [25] D. Aharonov and A. Ta-Shma, Adiabatic quantum state generation and statistical zero knowledge, in *Proceedings of the thirty-fifth annual ACM symposium on Theory of computing* (2003) pp. 20–29.
- [26] A. Aspuru-Guzik, A. D. Dutoi, P. J. Love, and M. Head-Gordon, Simulated quantum computation of molecular energies, *Science* **309**, 1704 (2005).
- [27] R. Cleve, A. Ekert, C. Macchiavello, and M. Mosca, Quantum algorithms revisited, *Proceedings of the Royal Society of London. Series A: Mathematical, Physical and Engineering Sciences* **454**, 339 (1998).
- [28] G.-L. Long and Y. Sun, Efficient scheme for initializing a quantum register with an arbitrary superposed state, *Physical Review A* **64**, 014303 (2001).
- [29] Y. Ge, J. Tura, and J. I. Cirac, Faster ground state preparation and high-precision ground energy estimation with fewer qubits, *Journal of Mathematical Physics* **60** (2019).
- [30] N. Gleinig and T. Hoefler, An efficient algorithm for sparse quantum state preparation, in *2021 58th ACM/IEEE Design Automation Conference (DAC)* (IEEE, 2021) pp. 433–438.
- [31] D. W. Berry, Y. Tong, T. Khattar, A. White, T. I. Kim, G. H. Low, S. Boixo, Z. Ding, L. Lin, S. Lee, *et al.*, Rapid initial-state preparation for the quantum simulation of strongly correlated molecules, *PRX Quantum* **6**, 020327 (2025).
- [32] D. Poulin and P. Wocjan, Preparing ground states of quantum many-body systems on a quantum computer, *Physical review letters* **102**, 130503 (2009).
- [33] A. Kandala, A. Mezzacapo, K. Temme, M. Takita, M. Brink, J. M. Chow, and J. M. Gambetta, Hardware-efficient variational quantum eigensolver for small molecules and quantum magnets, *nature* **549**, 242 (2017).
- [34] M. Cerezo, K. Sharma, A. Arrasmith, and P. J. Coles, Variational quantum state eigensolver, *npj Quantum Information* **8**, 113 (2022).
- [35] D. Gross, Y.-K. Liu, S. T. Flammia, S. Becker, and J. Eisert, Quantum state tomography via compressed sensing, *Physical review letters* **105**, 150401 (2010).
- [36] S. T. Flammia, D. Gross, Y.-K. Liu, and J. Eisert, Quantum tomography via compressed sensing: error bounds, sample complexity and efficient estimators, *New Journal of Physics* **14**, 095022 (2012).
- [37] R. Kueng, H. Rauhut, and U. Terstiege, Low rank matrix recovery from rank one measurements, *Applied and Computational Harmonic Analysis* **42**, 88 (2017).

- [38] K. Stannigel, P. Hauke, D. Marcos, M. Hafezi, S. Diehl, M. Dalmonte, and P. Zoller, Constrained dynamics via the zeno effect in quantum simulation: Implementing non-abelian lattice gauge theories with cold atoms, *Physical review letters* **112**, 120406 (2014).
- [39] L. Tarruell and L. Sanchez-Palencia, Quantum simulation of the hubbard model with ultracold fermions in optical lattices, *Comptes Rendus Physique* **19**, 365 (2018).
- [40] T. Hensgens, T. Fujita, L. Janssen, X. Li, C. Van Diepen, C. Reichl, W. Wegscheider, S. Das Sarma, and L. M. Vandersypen, Quantum simulation of a fermi–hubbard model using a semiconductor quantum dot array, *Nature* **548**, 70 (2017).
- [41] W. J. Huggins, O. Leimkuhler, T. F. Stetina, and K. B. Whaley, Efficient state preparation for the quantum simulation of molecules in first quantization, *PRX Quantum* **6**, 020319 (2025).
- [42] M. Greiner, O. Mandel, T. Esslinger, T. W. Hänsch, and I. Bloch, Quantum phase transition from a superfluid to a mott insulator in a gas of ultracold atoms, *nature* **415**, 39 (2002).
- [43] C. Nayak, S. H. Simon, A. Stern, M. Freedman, and S. Das Sarma, Non-abelian anyons and topological quantum computation, *Reviews of Modern Physics* **80**, 1083 (2008).
- [44] S. Bravyi and D. Gosset, Improved classical simulation of quantum circuits dominated by clifford gates, *Physical review letters* **116**, 250501 (2016).
- [45] S. Bravyi, D. Browne, P. Calpin, E. Campbell, D. Gosset, and M. Howard, Simulation of quantum circuits by low-rank stabilizer decompositions, *Quantum* **3**, 181 (2019).
- [46] J. Sun, L. Cheng, and S.-X. Zhang, Stabilizer ground states for simulating quantum many-body physics: theory, algorithms, and applications, *Quantum* **9**, 1782 (2025).
- [47] D. Gottesman, The heisenberg representation of quantum computers, *arXiv preprint quant-ph/9807006* (1998).
- [48] S. Aaronson and D. Gottesman, Improved simulation of stabilizer circuits, *Physical Review A—Atomic, Molecular, and Optical Physics* **70**, 052328 (2004).
- [49] E. T. Campbell, B. M. Terhal, and C. Vuillot, Roads towards fault-tolerant universal quantum computation, *Nature* **549**, 172 (2017).
- [50] M. Howard and E. Campbell, Application of a resource theory for magic states to fault-tolerant quantum computing, *Phys. Rev. Lett.* **118**, 090501 (2017).
- [51] M. Motta, C. Sun, A. T. Tan, M. J. O’Rourke, E. Ye, A. J. Minnich, F. G. Brandao, and G. K.-L. Chan, Determining eigenstates and thermal states on a quantum computer using quantum imaginary time evolution, *Nature Physics* **16**, 205 (2020).
- [52] S. McArdle, T. Jones, S. Endo, Y. Li, S. C. Benjamin, and X. Yuan, Variational ansatz-based quantum simulation of imaginary time evolution, *npj Quantum Information* **5**, 75 (2019).
- [53] S.-N. Sun, M. Motta, R. N. Tazhigulov, A. T. Tan, G. K.-L. Chan, and A. J. Minnich, Quantum computation of finite-temperature static and dynamical properties of spin systems using quantum imaginary time evolution, *PRX Quantum* **2**, 010317 (2021).
- [54] M. Cerezo, A. Arrasmith, R. Babbush, S. C. Benjamin, S. Endo, K. Fujii, J. R. McClean, K. Mitarai, X. Yuan, L. Cincio, *et al.*, Variational quantum algorithms, *Nature Reviews Physics* **3**, 625 (2021).
- [55] J. Biamonte, Universal variational quantum computation, *Physical Review A* **103**, L030401 (2021).
- [56] J. Tilly, H. Chen, S. Cao, D. Picozzi, K. Setia, Y. Li, E. Grant, L. Wossnig, I. Rungger, G. H. Booth, *et al.*, The variational quantum eigensolver: a review of methods and best practices, *Physics Reports* **986**, 1 (2022).
- [57] Y. Mao, M. Chaudhary, M. Kondappan, J. Shi, E. O. Ilo-Okeke, V. Ivannikov, and T. Byrnes, Measurement-based deterministic imaginary time evolution, *Physical Review Letters* **131**, 110602 (2023).
- [58] M. Suzuki, Improved trotter-like formula, *Physics Letters A* **180**, 232 (1993).
- [59] H. F. Trotter, On the product of semi-groups of operators, *Proceedings of the American Mathematical Society* **10**, 545 (1959).
- [60] E. Kapit, P. Ginsparg, and E. Mueller, Non-abelian braiding of lattice bosons, *Physical Review Letters* **108**, 066802 (2012).
- [61] E. O. Ilo-Okeke, Y. Ji, P. Chen, Y. Mao, M. Kondappan, V. Ivannikov, Y. Xiao, and T. Byrnes, Deterministic preparation of supersinglets with collective spin projections, *Physical Review A* **106**, 033314 (2022).
- [62] M. Kondappan, M. Chaudhary, E. O. Ilo-Okeke, V. Ivanikov, and T. Byrnes, Imaginary-time evolution with quantum nondemolition measurements: Multiqubit interactions via measurement nonlinearities, *Physical Review A* **107**, 042616 (2023).
- [63] T. Chen and T. Byrnes, Efficient preparation of the aklt state with measurement-based imaginary time evolution, *Quantum* **8**, 1557 (2024).
- [64] D. Gottesman, A class of quantum error-correcting codes saturating the quantum hamming bound, *arXiv preprint quant-ph/9604038* (1996).
- [65] D. Gottesman, *Stabilizer codes and quantum error correction* (California Institute of Technology, 1997).
- [66] R. Laflamme, C. Miquel, J. P. Paz, and W. H. Zurek, Perfect quantum error correcting code, *Physical Review Letters* **77**, 198 (1996).
- [67] A. Y. Kitaev, Quantum computations: algorithms and error correction, *Russian Mathematical Surveys* **52**, 1191 (1997).
- [68] D. Gottesman, An introduction to quantum error correction and fault-tolerant quantum computation, *arXiv preprint arXiv:0904.2557* (2009).
- [69] R. Sarkar and E. van den Berg, On sets of maximally commuting and anticommuting pauli operators, *Research in the Mathematical Sciences* **8**, 14 (2021).
- [70] M. Leonetti, *A Deterministic Decoration Scheme for Measurement-Based Variational Quantum Eigensolvers*, Ph.D. thesis, Politecnico di Torino (2025).
- [71] N. De Beaudrap, A linearized stabilizer formalism for systems of finite dimension, *arXiv preprint arXiv:1102.3354* (2011).
- [72] C. Gidney, Stim: a fast stabilizer circuit simulator, *Quantum* **5**, 497 (2021).
- [73] S. Masot-Llima and A. Garcia-Saez, Stabilizer tensor networks: Universal quantum simulator on a basis of stabilizer states, *Physical Review Letters* **133**, 230601 (2024).
- [74] R. S. Bennink, E. M. Ferragut, T. S. Humble, J. A. Laska, J. J. Nutaro, M. G. Pleszkoch, and R. C. Pooser, Unbiased simulation of near-clifford quantum circuits, *Physical Review A* **95**, 062337 (2017).

- [75] H. Hamaguchi, K. Hamada, and N. Yoshioka, Handbook for quantifying robustness of magic, *Quantum* **8**, 1461 (2024).
- [76] Q. Wu and J.-K. Hao, A review on algorithms for maximum clique problems, *European Journal of Operational Research* **242**, 693 (2015).
- [77] U. Feige, Approximating maximum clique by removing subgraphs, *SIAM Journal on Discrete Mathematics* **18**, 219 (2004).
- [78] S. Butenko, *Maximum independent set and related problems, with applications* (University of Florida, 2003).
- [79] Q. Wu and J.-K. Hao, An adaptive multistart tabu search approach to solve the maximum clique problem, *Journal of Combinatorial Optimization* **26**, 86 (2013).
- [80] J. Cheng, Y. Ke, A. W.-C. Fu, J. X. Yu, and L. Zhu, Finding maximal cliques in massive networks, *ACM Transactions on Database Systems (TODS)* **36**, 1 (2011).
- [81] G. Chapuis, H. Djidjev, G. Hahn, and G. Rizk, Finding maximum cliques on a quantum annealer, in *Proceedings of the Computing Frontiers Conference* (2017) pp. 63–70.
- [82] R. Herrman, L. Treffert, J. Ostrowski, P. C. Lotshaw, T. S. Humble, and G. Siopsis, Impact of graph structures for qaoa on maxcut, *Quantum Information Processing* **20**, 289 (2021).
- [83] P. Guturu and R. Dantu, An impatient evolutionary algorithm with probabilistic tabu search for unified solution of some np-hard problems in graph and set theory via clique finding, *IEEE Transactions on Systems, Man, and Cybernetics, Part B (Cybernetics)* **38**, 645 (2008).
- [84] A. F. Shaw, P. Lougovski, J. R. Stryker, and N. Wiebe, Quantum algorithms for simulating the lattice schwinger model, *Quantum* **4**, 306 (2020).
- [85] B. Chakraborty, M. Honda, T. Izubuchi, Y. Kikuchi, and A. Tomiya, Classically emulated digital quantum simulation of the schwinger model with a topological term via adiabatic state preparation, *Physical Review D* **105**, 094503 (2022).
- [86] C. Damm, Problems complete for $\oplus 1$, in *Aspects and Prospects of Theoretical Computer Science: 6th International Meeting of Young Computer Scientists Smolenice, Czechoslovakia, November 19–23, 1990 Proceedings 6* (Springer, 1990) pp. 130–137.
- [87] M. Nest, Classical simulation of quantum computation, the gottesman-knill theorem, and slightly beyond, arXiv preprint arXiv:0811.0898 (2008).
- [88] M. Heyl, A. Polkovnikov, and S. Kehrein, Dynamical quantum phase transitions in the transverse-field ising model, *Physical review letters* **110**, 135704 (2013).
- [89] N. Mohseni, P. L. McMahon, and T. Byrnes, Ising machines as hardware solvers of combinatorial optimization problems, *Nature Reviews Physics* **4**, 363 (2022).